Energy Fuels **2009,** *23,* 5092–5098 · DOI:10.1021/ef9005252
Published on Web 08/26/2009

energy&fuels
article

Analysis of a Plate-Type Microreformer for Methanol Steam Reforming Reaction

Falin Chen,[†] Min-Hsing Chang,*[,‡] Chih-Yi Kuo,[†] Ching-Yi Hsueh,[§] and We-Mon Yan[∥]

[†]*Institute of Applied Mechanics, National Taiwan University, Taipei 106, Taiwan, Republic of China,* [‡]*Department of Mechanical Engineering, Tatung University, Taipei 104, Taiwan, Republic of China,* [§]*Department of Mechanical Engineering, National Chiao Tung University, Hsin-Chu, 300, Taiwan, Republic of China, and* [∥]*Department of Mechatronic Engineering, Huafan University, Taipei 223, Taiwan, Republic of China*

Received May 25, 2009. Revised Manuscript Received July 23, 2009

A numerical simulation is performed in this study for a plate-type microreactor with parallel microchannels and diagonal inlets/outlets. The methanol steam reforming reaction is considered, and the performance is evaluated by examining the concentration profiles of methanol, hydrogen, and carbon monoxide within the rector under various operating conditions, including the influences of the steam/carbon (S/C) ratio, reaction temperature, and liquid feed rate. Particularly, the effect of aspect ratio of the microchannel on the methanol conversion rate, hydrogen generation rate, and mole fraction of carbon monoxide in the outlet gas mixture are also explored. The results show that such a plate-type design of methanol microreformer may cause nonuniform reaction states in each microchannel and affect its reforming performance significantly. It is found that these concentration nonuniformities are heavily dependent on the reaction temperature, S/C ratio, and liquid feed rate. The numerical model provides an efficient way to characterize the reforming reactions within the reactor, and the results will benefit the future design for a plate-type methanol microreformer.

1. Introduction

Applications of fuel cells in portable power sources have received much attention, especially for polymer electrolyte fuel cells (PEFCs) and direct methanol fuel cells (DMFCs), because of their low operating temperature and rapid start-up performance. However, the volumetric energy density of hydrogen is relatively lower, which makes it difficult to reduce the volume of fuel storage system in practical applications of portable PEFCs. For DMFCs, the liquid methanol possesses higher volumetric energy density while the system requires higher catalyst loading, and the fuel crossover phenomenon is still difficult to overcome. Although this problem can be improved using a dilute methanol solution, it decreases the energy density and also increases the design complexity of fuel system simultaneously. To solve this technical difficulty, one possible solution is the employment of a methanol microreformer. The liquid methanol first passes through the microreformer and then the generating hydrogen flows directly into the PEFC. Such a design combines the merits of PEFCs and DMFCs: using methanol as high volumetric energy density fuel and producing the same level of performance in power output as PEFCs.

Numerous studies have been devoted to the investigation of micro fuel reactors for methanol steam reforming in the literature.[1−30] Detailed reviews for this research field can be

*Author to whom correspondence should be addressed. E-mail: mhchang@ttu.edu.tw.

(1) Holladay, J. D.; Wang, Y.; Jones, E. *Chem. Rev.* **2004**, *104*, 4767–4790.
(2) Palo, D. R.; Dagle, R. A.; Holladay, J. D. *Chem. Rev.* **2007**, *107*, 3992–4021.
(3) Palo, D. R.; Holladay, J. D.; Rozmiarek, R. T.; Leong, C. E. G.; Wang, Y.; Hu, J.; Chin, Y. H.; Dagle, R. A.; Baker, E. G. *J. Power Sources* **2002**, *108*, 28–34.
(4) Holladay, J. D.; Jones, E. O.; Dagle, R. A.; Xia, G. G.; Cao, C.; Wang, Y. *J. Power Sources* **2004**, *131*, 69–72.
(5) Minsker, L. K.; Renken, A. *Catal. Today* **2005**, *110*, 2–14.
(6) Xia, G.; Holladay, J. D.; Dagle, R. A.; Jones, E. O.; Wang, Y. *Chem. Eng. Technol.* **2005**, *28*, 515–519.
(7) Kawamura, Y.; Yamamoto, K.; Ogura, N.; Katsumata, T.; Igarashi, A. *J. Power Sources* **2005**, *150*, 20–26.
(8) Huang, C. Y.; Sun, Y. M.; Chou, C. Y.; Su, C. C. *J. Power Sources* **2007**, *166*, 450–457.
(9) Seo, D. J.; Yoon, W. L.; Yoon, Y. G.; Park, S. H.; Park, G. G.; Kim, C. S. *Electrochim. Acta* **2004**, *50*, 719–723.
(10) Park, G. G.; Yim, S. D.; Yoon, Y. G.; Kim, C. S. *Catal. Today* **2005**, *110*, 108–113.
(11) Park, G. G.; Yim, S. D.; Yoon, Y. G.; Lee, W. Y.; Kim, C. S.; Seo, D. J.; Eguchi, K. *J. Power Sources* **2005**, *145*, 702–706.
(12) Lim, M. S.; Kim, M. R.; Noh, J.; Woo, S. I. *J. Power Sources* **2005**, *140*, 66–71.
(13) Shah, K.; Ouyang, X.; Besser, R. S. *Chem. Eng. Technol.* **2005**, *28*, 303–313.
(14) Kwon, O. J.; Hwang, S. M.; Ahn, J. G.; Kim, J. J. *J. Power Sources* **2006**, *156*, 253–259.
(15) Jeong, H.; Kim, K. I.; Kim, T. H.; Ko, C. H.; Park, H. C.; Song, I. K. *J. Power Sources* **2006**, *159*, 1296–1299.
(16) Kim, T.; Kwon, S. *J. Micromech. Microeng.* **2006**, *16*, 1760–1768.
(17) Kim, T.; Kwon, S. *Chem. Eng. J.* **2006**, *123*, 93–102.
(18) Yoshida, K.; Tanaka, S.; Hiraki, H.; Esashi, M. *J. Micromech. Microeng.* **2006**, *16*, S191–S197.
(19) Shin, Y.; Kim, O.; Hong, J. C.; Oh, J. H.; Kim, W. J.; Haam, S.; Chung, C. H. *Int. J. Hydrogen Energy* **2006**, *31*, 1925–1933.
(20) Kawamura, Y.; Ogura, N.; Yamamoto, T.; Igarashi, A. *Chem. Eng. Sci.* **2006**, *61*, 1092–1101.
(21) Won, J. Y.; Jun, H. K.; Jeon, M. K.; Woo, S. I. *Catal. Today* **2006**, *111*, 158–163.
(22) Sohn, J. M.; Byun, Y. C.; Cho, J. Y.; Choe, J.; Song, K. H. *Int. J. Hydrogen Energy* **2007**, *32*, 5103–5108.
(23) Kundu, A.; Park, J. M.; Ahn, J. E.; Park, S. S.; Shul, Y. G.; Han, H. S. *Fuel* **2007**, *86*, 1331–1336.
(24) Stefanescu, A.; van Veen, A. C.; Mirodatos, C.; Beziat, J. C.; Brunel, E. D. *Catal. Today* **2007**, *125*, 16–23.
(25) Kundu, A.; Ahn, J. E.; Park, S. S.; Shul, Y. G.; Han, H. S. *Chem. Eng. J.* **2008**, *135*, 113–119.
(26) Choi, Y.; Stenger, H. G. *J. Power Sources* **2003**, *124*, 432–439.
(27) Cao, C.; Wang, Y.; Holladay, J. D.; Jones, E. O.; Palo, D. R. *AIChE J.* **2005**, *51*, 982–988.
(28) Cominos, V.; Hardt, S.; Hessel, V.; Kolb, G.; Lowe, H.; Wichert, M.; Zapf, R. *Chem. Eng. Commun.* **2005**, *192*, 685–698.
(29) Pan, L.; Wang, S. *Chem. Eng. J.* **2005**, *108*, 51–58.
(30) Purnama, H.; Ressler, T.; Jentoft, R. E.; Soerijanto, H.; Schlogl, R.; Schomacker, R. *Appl. Catal., A* **2004**, *259*, 83–94.

found in the work of Holladay and co-workers.[1,2] Particularly, the plane-type microreactors have received much attention, because of their compact sizes and great potential to be used in portable fuel cell systems as a hydrogen generation unit.[9−25] Seo et al.[9] used stainless steel as a substrate to fabricate a unit of reformer and vaporizer. The heat for the endothermic reaction originates from an electric heater, and the developed fuel processor can generate sufficient hydrogen for a fuel cell with a power output of 10 W. Park and coworkers[10,11] also developed a microchannel methanol steam reformer. The system is comprised of a fuel vaporizer, a heat exchanger, a catalytic combustor, and a steam reformer. They found that the microchannel patterning, the catalyst coating, and the microchannel bonding can significantly affect the reactor performance. Lim et al.[12] fabricated a plate-type reactor with 10 parallel channels on a stainless steel substrate. They found that the catalyst coated with a zirconia-sol solution exhibited good adherence on the substrate. The challenges and prospects for micro fuel processors were proposed by Shah et al.[13] They suggested that the microreaction technology is the most promising method of supplying hydrogen for feeding portable fuel cells. Kwon et al.[14] made a microreformer using a silicon wafer substrate and a "fill-and-dry" method for catalyst coating. The stack of microreformer only occupies 15 cm^3, and the maximum hydrogen production rate occurs at ~320 °C in their experiments. In contrast to the widely used commercial Cu-ZnO-Al_2O_3 catalyst, Jeong et al.[15] studied the steam reforming of methanol over a series of Cu/Zn-based catalysts by a microchannel reactor. They found that a microreactor coated with Cu/ZnO/ZrO_2/Al_2O_3 catalyst with an undercoated Al_2O_3 buffer layer exhibits a higher methanol conversion rate and a lower CO concentration in the outlet gas. Kim and Kwon[16] designed a multichannel catalytic microreactor by anisotropic wet etching of photosensitive glass and established the overall fabrication processes for a microelectromechanical systems (MEMS)-based design. They further discussed the fabrication procedures for a methanol microreformer, including catalyst preparation, coating, and patterning on a wafer.[17] A microreformer integrated with a combustor and an evaporator was developed by Yoshida et al.[18] They found that the design of the microchannel evaporator is critical to obtain larger hydrogen output. Shin et al.[19] also designed a micro fuel processor system using low-temperature cofired ceramics and considered both steam reforming and partial oxidation processes. Kawamura et al.[20] fabricated a methanol microreformer by glass and silicon substrates. A serpentine catalyst-coated microchannel was designed based on a simple one-dimensional theoretical model. A microchannel reactor with combustor for methanol steam reforming was designed by Won et al.[21] They found that the temperature of the combustor could be controlled, depending on the methanol feed rate. A plate-type fuel processor was developed by Sohn et al.[22] for a 150-W polymer exchange membrane (PEM) fuel cell system. The fuel processor includes a reformer, a combustor, a heat exchanger, and a evaporator and could be operated without any external heat supply. Kundu et al.[23] studied the stability and performance of a microchannel reactor for methanol steam reforming with different sols as a binder in the catalyst coating. They found that the mixed sol of alumina and zirconia comparatively produced better performance. Stefanescu et al.[24] developed the suspension coating method using alumina prepared from commercial powders and studied the optimization of wall coating for microchannel reactors. Recently, Kundu et al.[25] further compared the performance and pressure drop of catalyst-coated and catalyst-packed microchannel reactors. They found that the pressure drop in a packed catalyst reactor is higher while the complete conversion of methanol could be achieved at lower temperature with a packed catalyst design.

So far, most studies have focused on the experimental measurements. Only limited studies pay attention to the development of a theoretical model and numerical simulation for methanol microreformers. Choi and Stenger[26] studied the water-gas shift reaction in the reforming system of the fuel cell and obtained an empirical rate expression from the experimental data, using nonlinear least-squares optimization. Cao et al.[27] described a cylindrical-type micro fuel processor and developed a three-dimensional pseudo-homogeneous model based on fundamental conservation laws of mass and energy. Their results provide carbon conversion and local temperature distribution in the micro fuel processor. Cominos et al.[28] fabricated a methanol microreformer and investigated its performance with different compositions and loadings of catalysts under various operating conditions. They also simulated the flow distribution pattern at the inlet and outlet sections of the device, using the commercial CFD-ACE+ software. Pan and Wang[29] designed a compact plate-fin methanol reformer in which the endothermic and exothermic reactions are integrated into one unit. Its performance was investigated by both experiment and numerical simulation. The theoretical predictions are in good agreement with experimental data, and the numerical model could accurately predict the methanol conversion and the reformate composition in the reacting chamber. Because the microreformer based on the plate-type design has been widely investigated experimentally, in this study, we develop a numerical model to simulate the plate-type microreformer for methanol steam reforming. Numerical simulations are performed to investigate the concentration distributions of methanol, hydrogen, and carbon monoxide in the reactor, with respect to the variations of liquid feed rate, reaction temperature, and steam/carbon (S/C) ratio. The effects of aspect ratio of the microchannel on the methanol conversion performance are also examined. Results provide numerical predictions for the concentration profiles of reactants and products in the system and benefit the further design of the plate-type methanol microreformer for practical application in portable fuel cell systems.

2. Theoretical Model and Formulation

The top view of the plate-type microreformer is shown in Figure 1. The reactor contains 10 parallel channels, each with a

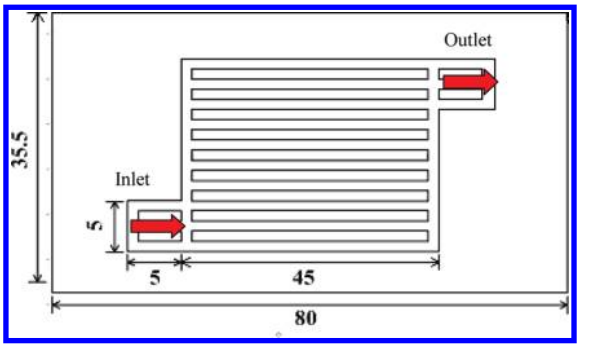

Figure 1. Top view of the plate-type microreactor (dimensions given in units of millimeters). The depth of the flow channel is 0.5 mm.

width of 1 mm. The mixture of methanol and steam enters the reactor and then the steam reforming reaction occurs when the mixture flows through the parallel microchannels. The outlet is in a diagonal position, with respect to the inlet. The surface of each microchannel is assumed to be coated with $Cu/ZnO/Al_2O_3$ catalyst with a thickness of 30 μm. To simplify the development of three-dimensional numerical model, we assume that the flow is incompressible and under steady state within the reactor. The mixture of gases behaves as an ideal gas, and the chemical reaction occurs only within the catalyst layer. The reactor is made of stainless steel, and the bottom surface is held at a fixed temperature. Accordingly, the governing equations, based on the platform of Fluent software, can be established to simulate the reaction of methanol steam reforming. The continuity and momentum equations are respectively given as

$$(\varepsilon\rho)\frac{\partial u_i}{\partial x_i} = 0 \tag{1}$$

$$\varepsilon u_j \frac{\partial u_i}{\partial x_j} = -\frac{\varepsilon}{\rho}\frac{\partial p}{\partial x_i} + \varepsilon\nu\frac{\partial^2 u_i}{\partial x_j^2} + S_i \tag{2}$$

where ε is the porosity, ρ the density, p the pressure, and ν the kinematic viscosity. The source term S_i in eq 2 is induced by the flow through the catalyst layer. Here, we use the model of porous media to simulate the catalyst layer, and this term is represented in the form

$$S_i = -\frac{\nu u_i}{k_p} - \frac{\beta u_i}{2}|u_j| \tag{3}$$

where k_p is the permeability and β is the inertial loss coefficient. Note that this source term vanishes in the domain of flow channel and exists only within the catalyst layer. The energy equation is

$$\rho c_p u_j \frac{\partial T}{\partial x_j} = k_{\text{eff}}\frac{\partial^2 T}{\partial {x_j}^2} + S_t \tag{4}$$

where k_{eff} is the effective thermal conductivity and S_t is the source term due to the chemical reactions in the catalyst layer. The effective thermal conductivity represents the volume average of the fluid conductivity and the solid conductivity in the following form:

$$k_{\text{eff}} = \varepsilon k_f + (1-\varepsilon)k_s \tag{5}$$

where k_f and k_s are the fluid and solid thermal conductivity, respectively. The source term can be expressed by

$$S_t = -\sum_i \left(\frac{h_i^\circ}{M_{w,i}} + \int_{T_{\text{ref}},i}^{T} c_{p,i}\,dT\right)(R_{i,r}) \tag{6}$$

where h_i° is the enthalpy of formation, $M_{w,i}$ the molecular weight, $R_{i,r}$ the volumetric generation rate, and the subscript "i" represents the reactant species. The concentration equation is written as

$$\varepsilon u_j \frac{\partial C_i}{\partial x_j} = D_{\text{eff}}\frac{\partial^2 C_i}{\partial {x_j}^2} + S_c \tag{7}$$

where D_{eff} is the effective concentration diffusion coefficient and S_c is the source term due to the steam reforming reaction. The kinetic model for methanol and steam mixture flowing over $Cu/ZnO/Al_2O_3$ catalyst contains two reactions as follows:

$$CH_3OH + H_2O \xrightarrow{k_1} CO_2 + 3H_2 \tag{8}$$

$$CO_2 + H_2 \underset{k_{-2}}{\overset{k_2}{\rightleftharpoons}} CO + H_2O \tag{9}$$

The first is the methanol steam reforming (SR) reaction and the second is the reverse water-gas shift (rWGS) reaction. The source term S_c in eq 7 satisfies the following relationship:

$$S_c = M_{w,i}\sum_{r=\text{SR, rWGS}}^{N_R} R_{i,r} \tag{10}$$

where N_R the number of chemical species in the SR and rWGS reactions. By employing the power rate law, the kinetic reaction parameters and the rate equations of these reactions are defined as follows:

$$r_{\text{SR}} = k_1 {C_{CH_3OH}}^{0.6} {C_{H_2O}}^{0.4}\, exp(-\frac{E_a^1}{RT}) \tag{11}$$

$$r_{rWGS} = k_2 C_{CO_2} C_{H_2}\, exp(-\frac{E_a^2}{RT}) - k_{-2} C_{CO} C_{H_2O}\, exp(-\frac{E_a^2}{RT}) \tag{12}$$

where E_a^1 = 76 kJ/mol and E_a^2 = 108 kJ/mol. Detailed discussions for the reaction rate constants, activation energy, and pre-exponential factor for SR and rWGS reactions could be found in the study of Purnama et al.[30]

To solve this numerical model, the boundary conditions must be specified appropriately. At the inlet of the reactor the velocity, the temperature and concentration of the methanol−steam mixture are specified. The pressure at the outlet is assumed to be equal to the atmospheric pressure. In the microreactor, the normal velocity, concentration, and temperature are assumed to be continuous across the interface between the fluid layer and the catalyst layer. On the interface between the catalyst layer and the substrate, the temperature is also continuous and the normal velocity is zero, since there is no flow across the solid boundary. Finally, the temperature of the substrate is specified as the wall temperature. The mathematical model has been solved by the finite-volume method using a first-order upwind scheme. Several grid structures with different grid numbers also have been tested, to ensure numerical accuracy and obtain converged results with reasonable CPU time consumption. Some of the parameters used in the simulations are listed in Table 1.

Table 1. Parameters Used in the Simulations

parameter	value
inlet gas temperature	140 °C
catalyst density	890 kg/m^3
catalyst layer porosity	0.38
catalyst permeability	2.38×10^{-12} m^2
inertial loss coefficient, β	7.9×10^5 m^{-1}

3. Results and Discussion

We first examine the effects of liquid feed rate on the concentration profiles of methanol, hydrogen, and carbon monoxide (CO) within the reactor ,and the results are shown, respectively, in Figures 2a, 2b, and 2c for the typical case with a reaction temperature of 260 °C and a steam/carbon (S/C) ratio of 1.5. Note that, in practical devices, the methanol solution in the liquid phase should be vaporized first in a vaporizer and then flows into the reactor. Thus, here, we use the liquid feed rate, which is generally used in related studies to indicate the mass flow rate. While, in the simulations, the methanol−steam mixture at the inlet is in the gas phase, with the same mass flow rate as the assigned liquid feed rate. When the flow rate is low, as shown in the 0.5 mL/h case, the steam reforming reaction mainly occurs within the entrance region and the methanol concentration decreases rapidly along the microchannels to the outlet, as shown in Figure 2a. This result indicates that we may obtain a high methanol conversion rate under low liquid feed rate, but the hydrogen generation rate

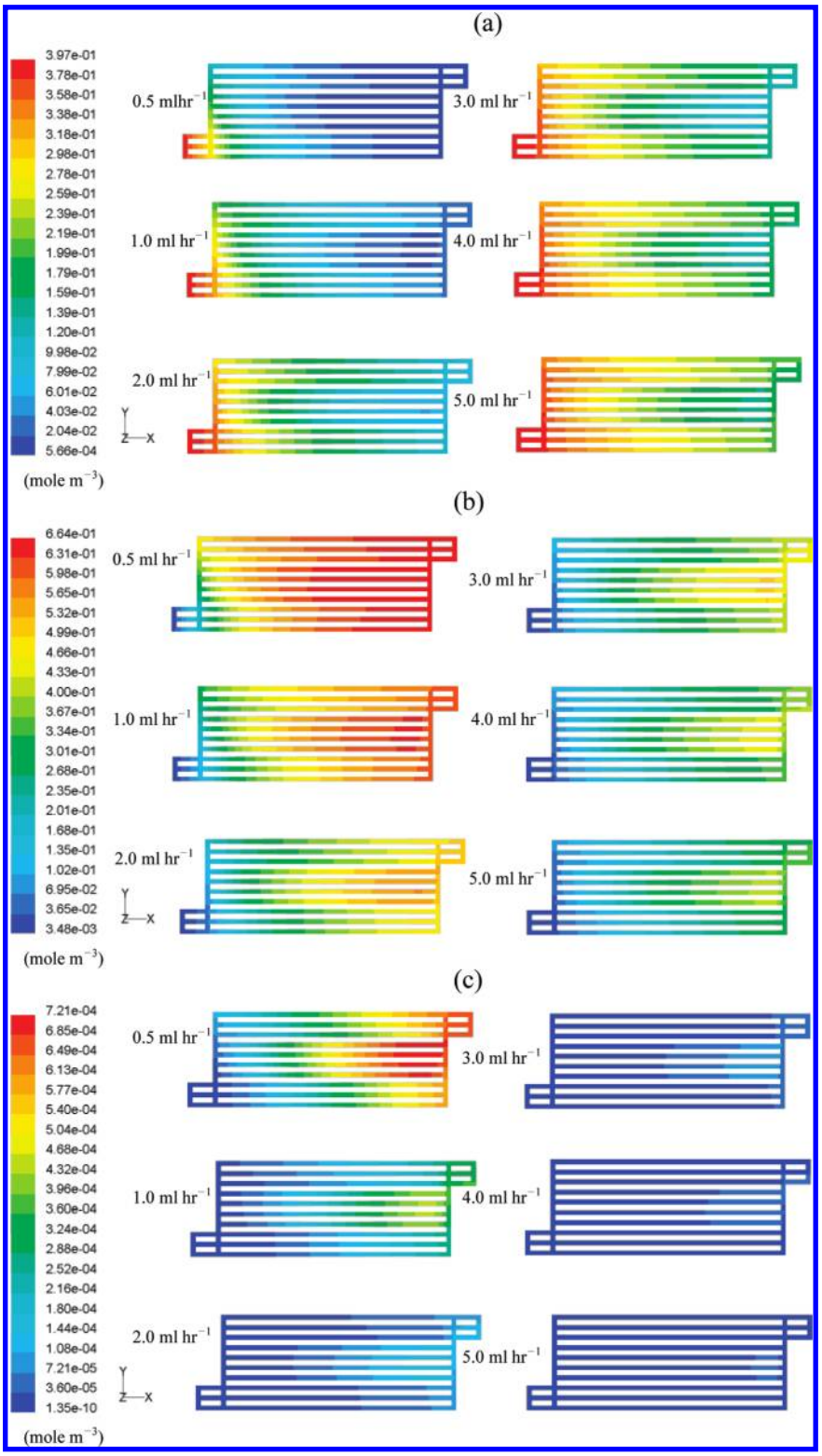

Figure 2. Concentration profiles of (a) methanol, (b) hydrogen, and (c) carbon monoxide for six assigned liquid feed rates with wall temperatures of 260 °C and a steam/carbon (S/C) ratio of 1.5.

also will be low, because of the low feed rate of the reactants. In addition, the utilization of reaction area is poor, because most of the regions of the reactor lack reactants to perform the reforming reaction. This condition can be improved gradually by increasing the liquid feed rate, as shown in the cases with a liquid feed rate of 1.0−5.0 mL/h. Apparently, with higher liquid feed rates, the reactants can reach the downstream area and make the reforming reaction more uniform within the reactor. Moreover, the hydrogen generation rate will also increase simultaneously, while the methanol conversion rate will decrease, because the methanol will pass through the reactor more quickly and have less time to come into contact with the catalyst layer. The decreasing rate of methanol concentration is also different in each microchannel.

One can see that the methanol conversion rate is higher in the central part of the reactor with such a diagonal inlet/outlet design. The concentration profiles of hydrogen are in contrast to those of methanol, as demonstrated in Figure 2b. In the case of low liquid feed rate (0.5 mL/h), the high methanol conversion rate results in high hydrogen concentration in the downstream area of the reactor. As the feed rate increases, the reduction in methanol conversion rate also causes the hydrogen concentration to decrease gradually, especially in the lower and upper parts of the reactor. The concentration of CO in the outlet gas mixture is also an important factor to evaluate the performance of a methanol reformer. If the concentration of CO is low enough, the outlet gas can be employed directly to the PEM fuel cells, especially the high-temperature PEM fuel cell systems using a polybenzimidazole (PBI) membrane with an operating temperature of > 120 °C, which possess a higher tolerance to the CO poisonous phenomena on the electrodes. As shown in Figure 2c, the CO concentration at the outlet is quite high at low liquid feed rates. That is, a higher methanol conversion rate is also in accordance with a higher CO concentration in the reactor, especially in the downstream parts of the central microchannels. It is also found that an increase in liquid feed rate is indeed an efficient way to reduce the CO generation rate and allow the outlet hydrogen-rich gas to be utilized directly for fuel cells.

The effects of temperature on the concentration profiles of methanol, hydrogen, and CO are respectively illustrated in Figure 3a, 3b, and 3c for three assigned wall temperatures with an S/C ratio of 1.5 and a liquid feed rate of 3 mL/h. We observe that the methanol conversion is quite poor at T_w = 220 °C, resulting in the low concentrations of hydrogen and CO within the reactor. Apparently, this condition can be improved by operating the reactor at higher wall temperature, as shown in the results for the cases with T_w = 260 and 300 °C. Because the liquid feed rates are the same, these results imply both the hydrogen generation rate and CO concentration in the outlet gas will be increased by raising the reaction temperature. It is also noted that the methanol conversion is relatively more efficient within the central microchannels and the CO is mainly generated in these regions. The reason is due to the microchannel design in the reactor. Obviously, under such a diagonal inlet/outlet design with parallel microchannels, the gas mixture is easier to pass through the reactor via the lower and upper microchannels and has less time to contact and react with the catalyst layer, causing a lower methanol conversion rate. Whereas, in the central microchannels, the gas mixture cannot reach the outlet directly and takes more time to flow through the reactor. Accordingly, it seems to have better conversion efficiency and produce higher CO concentration in these regions. These results show that this design of microreactor with parallel microchannels could be improved further to obtain more uniform concentration distributions and increase the reforming efficiency. One possible solution is to adopt the design with parallel-serpentine microchannels, which could be verified further in future theoretical study.

It is also important to explore the concentration profiles of methanol, hydrogen, and CO in the microreactor under different S/C ratio conditions. The results are respectively demonstrated in Figure 4a, 4b, and 4c with a liquid feed rate of 3 mL/h at T_w = 260 °C. As seen in Figure 4a, the region of high methanol concentration near the inlet recedes gradually and in Figure 4b, the mole fraction of hydrogen in the region

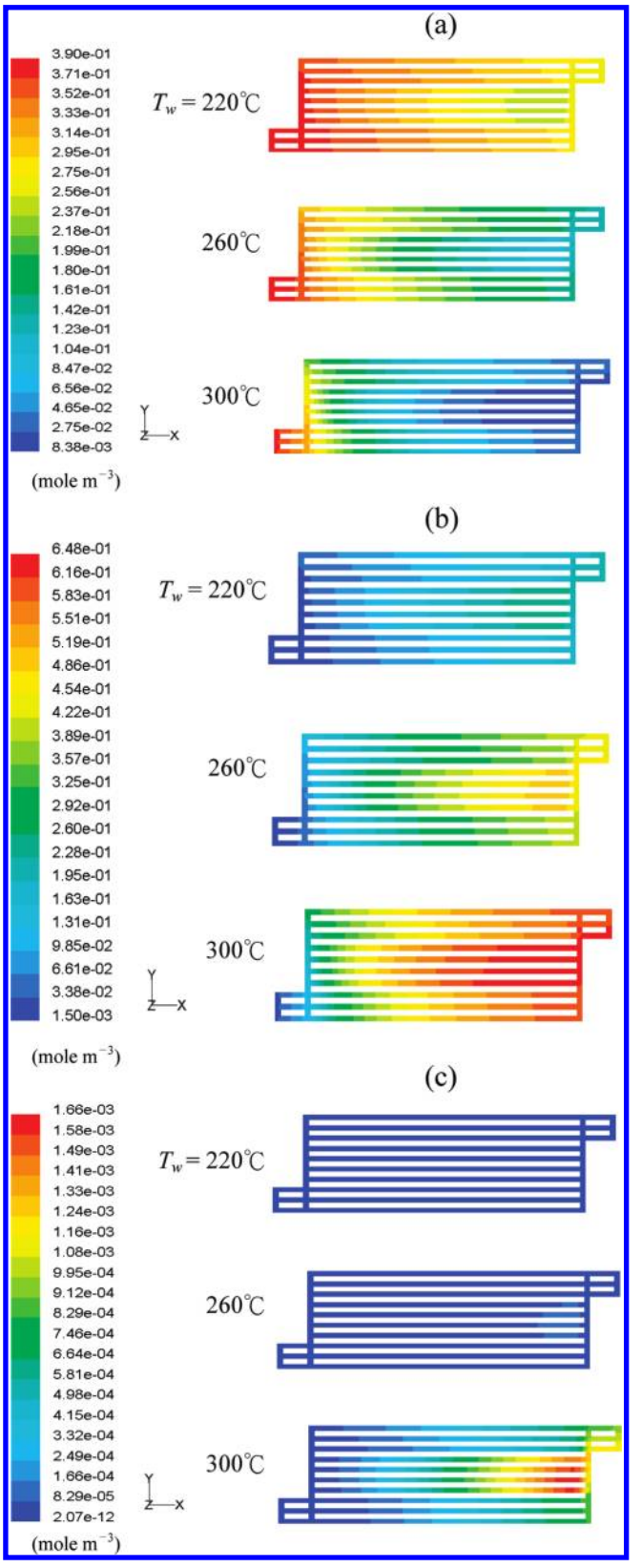

Figure 3. Concentration profiles of (a) methanol, (b) hydrogen, and (c) CO for three assigned wall temperatures with a S/C ratio of 1.5 and a liquid feed rate of 3 mL/h.

near the outlet reduces gradually with increasing S/C ratio, which are both due to the addition of steam (in terms of mole fraction) in the inlet gas mixture. It is obvious that the methanol conversion rate will be enhanced with higher S/C

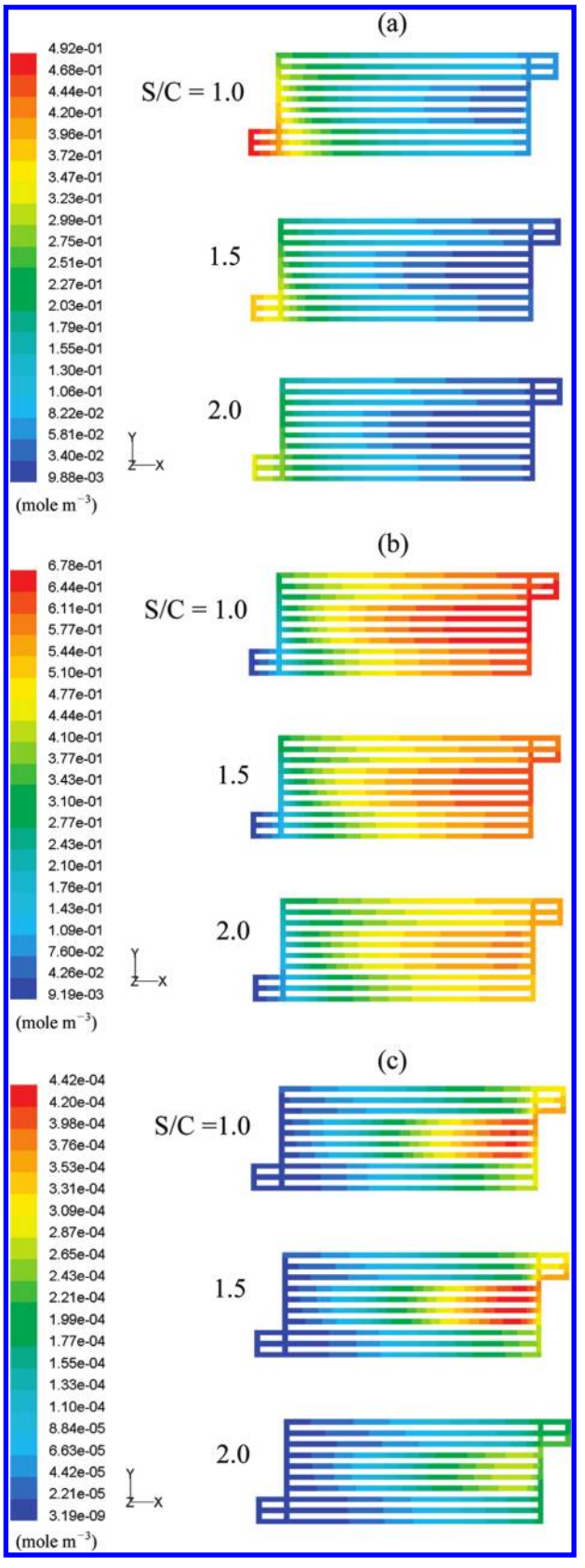

Figure 4. Concentration profiles of (a) methanol, (b) hydrogen, and (c) CO for three assigned S/C ratios with T_w = 260 °C and a liquid feed rate of 3 mL/h.

ratio. However, the case with an S/C ratio of 1.0 will still produce the highest hydrogen generation rate in these cases since the concentration of methanol is the highest under the

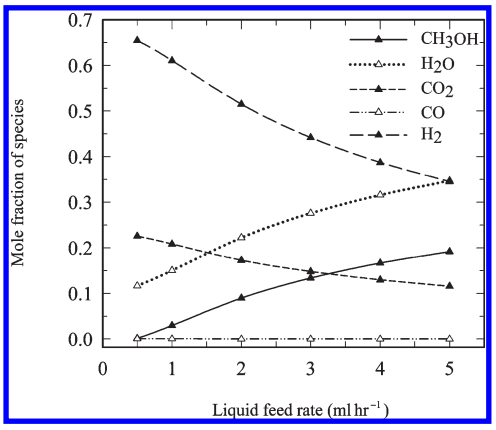

Figure 5. Mole fraction of all species in the outlet gas at T_w = 260 °C with an S/C ratio of 1.5.

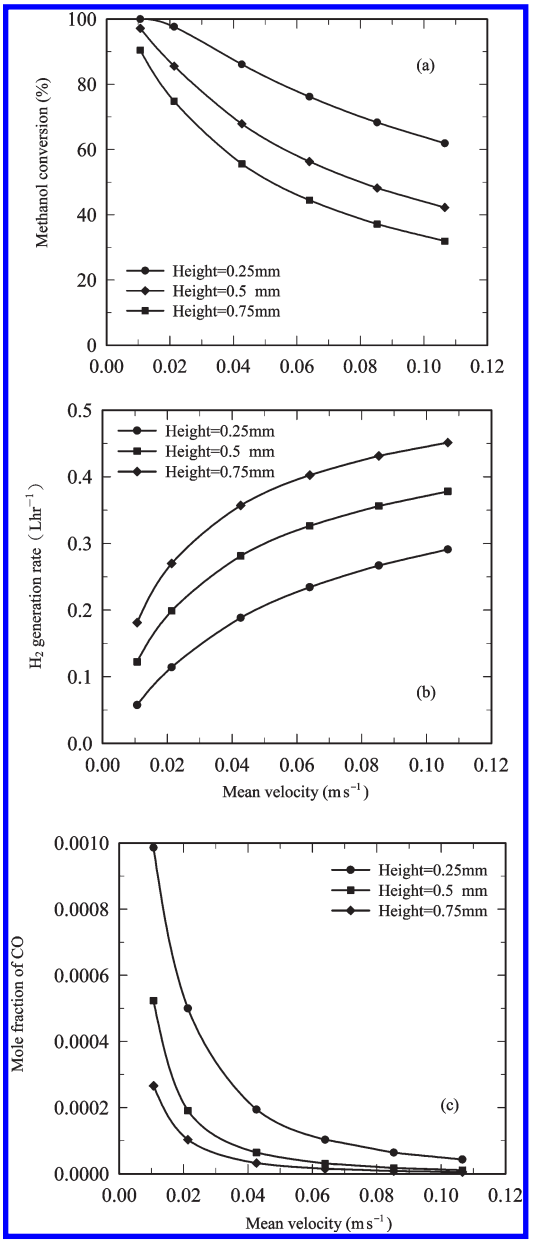

Figure 6. Variations of (a) the methanol conversion, (b) the hydrogen generation rate, and (c) the mole fraction of CO, for three assigned channel heights with T_w = 260 °C and an S/C ratio of 1.5.

same feeding rate. That is, in order to obtain sufficient hydrogen generation rate and high methanol conversion rate, the microreactor should operate with higher S/C ratio and liquid feed rate. Note that the central microchannels always generate more hydrogen. The higher hydrogen concentration in this region will enhance the rWGS reaction. Therefore, more CO will be produced in this region, as shown in Figure 4c. Because of the same mechanism in the central microchannels, the CO concentration seems to be reduced gradually with higher S/C ratio.

The variations of the mole fractions of all species with liquid feed rate are demonstrated in Figure 5 for a typical case with an S/C ratio of 1.5 and wall temperatures of 260 °C. It is found that the mole fraction of hydrogen decreases gradually as the liquid feed rate increases. Because the mole fraction of hydrogen is heavily dependent on the methanol conversion rate, as we have discussed in the results of Figure 2, an increase in liquid feed rate diminishes the methanol conversion rate and thus reduces the hydrogen concentration in the outlet gas simultaneously. A lower methanol conversion rate also results in a higher mole fraction of steam in the outlet gas. Therefore, the humidity of the hydrogen-rich gas mixture could be raised by increasing the liquid feed rate, especially when the gas mixture must be cooled to the proper temperature for the following application in fuel cells.

The aspect ratio of the cross section of the microchannel also may play an important role in the factors that affect the performance of the microreactor. To investigate this effect, we fix the microchannel width and adjust the aspect ratio (height/width) of the microchannel with different heights. In this way, the cross-sectional area will change and the mean velocity in the microchannel, with lower aspect ratio, will increase under the same liquid feed rate. To evaluate this effect reasonably, the liquid feed rate is replaced by the mean velocity at the inlet and the variations of methanol conversion, hydrogen generation rate, and CO concentration with the mean velocity are demonstrated in Figure 6a, 6b, and 6c, respectively, for three assigned microchannel heights. It is found that a lower aspect ratio gives significantly higher methanol conversion for the same mean velocities, as shown in Figure 6a, whereas a lower aspect ratio also indicates a smaller cross-sectional area, which results in a lower mass flow rate. Therefore, the hydrogen generation rate seems to decrease with lower microchannel height, as illustrated in Figure 6b. The microchannel height also affects the CO concentration in the outlet gas significantly, as shown in Figure 6c. For an assigned mean velocity, the CO concentration decreases quickly as the microchannel height increases. The results reveal that a higher methanol conversion also induces higher CO concentration and the adjustment of microchannel height seems to be a possible way to control the CO concentration in the outlet gas.

4. Conclusions

In this study, we have implemented a numerical study to simulate the performance of a plate-type microreformer constructed by parallel microchannels with a diagonal inlet/outlet design for the methanol steam reforming reaction. The effects of liquid feed rate, reaction temperature, and steam-to-carbon (S/C) ratio on the concentration profiles of methanol, hydrogen, and carbon monoxide (CO) within the reactor are explored, and the influences of aspect ratio of microchannel on the methanol conversion rate, hydrogen generation rate, and CO concentration in the outlet gas are examined in detail. The results show that the reforming reaction is not uniform in the microreactor and the microchannels in the central part always exhibit better reforming performance. Thus, the flow channel design should be improved further, to obtain more-uniform reaction conditions in each channel and higher reforming efficiency in finite volumetric space, and then we can get hydrogen-rich gas from a device occupying a smaller volume. From the CO concentration profiles, it is noted that the region with high methanol conversion also causes high CO concentration there and, thus, increases the CO concentration in the outlet gas. To reduce CO concentration, the microreactor should operate at lower temperature, higher liquid feed rate, and larger S/C and aspect ratios. According to the numerical results, a device of CO remover seems to be necessary if the outlet gas generated from this design is used as fuel for general polymer exchange membrane (PEM) fuel cell systems. A future theoretical study for different microchannel pattern will be beneficial for the optimization of methanol microreformer.

Note Added after ASAP Publication. The affiliations of the authors have been modified. The original version of the paper was posted to the Web on August 26. The revised version of the paper was reposted to the Web on September 4.

Acknowledgment. The financial support from National Science Council of Taiwan (through Grant No. NSC 96-2221-E-036-041) is gratefully acknowledged.